IET Microwaves, Antennas & Propagation

Research Article

Broadband planar slot antenna using a simple single-layer FSS stopband

ISSN 1751-8725
Received on 11th May 2019
Revised 23rd November 2019
Accepted on 4th December 2019
doi: 10.1049/iet-map.2019.0365
www.ietdl.org

Djaouida Belmessaoud[1] ✉, Khaled Rouabah[2], Idris Messaoudene[2,3], Tayeb A. Denidni[4]
[1]*Electronics Department, University of M'sila, M'Sila 28000, Algeria*
[2]*LETA, Electronics Department, University of Bordj Bou Arreridj, El Anasser 34031, Algeria*
[3]*Ecole Nationale Supérieure d'Informatique (ESI ex. INI), Algiers, Algeria*
[4]*EMT-INRS, Institut National de la Recherche Scientifique, Quebec City, Canada*
✉ *E-mail: djaouida.belmessaoud@univ-msila.dz*

Abstract: In this study, the authors propose a simple structure of a new broadband planar slot antenna using a wide single-layer frequency selective surface (FSS) stopband. The proposed design is realised in two stages. First, the performances of the FSS unit cells are investigated using the finite element method of high-frequency structure simulator. Besides, the FSS structure considered as a stop-band filter in the bandwidth $(3-7\,\text{GHz})$, is also validated by computer simulation technology microwave studio. Second, this FSS reflector is combined with a miniaturised wideband planar slot antenna $(29\times 24\times 1.57\ \text{mm}^3)$. The final proposed combination is also designed, optimised, fabricated and validated by measurements. The obtained results show an operating impedance bandwidth of 86.38% $(2.92-7.36\,\text{GHz})$ including the Worldwide interoperability for Microwave Access band, the C band for satellite applications, and the Wireless Local Area Network band. Furthermore, the antenna provides an $8.87\,\text{dBi}$ measured maximum gain. Compared to the same antenna without FSS, a maximum gain enhancement of $5.53\,\text{dBi}$ is achieved by the proposed structure. In addition, the back lobes are reduced in the proposed structure by $>15\,\text{dBi}$, compared to a simple antenna. The total size of the proposed antenna, integrating the FSS, is $0.63\lambda_0\times 0.63\lambda_0\times 0.12\lambda_0$.

1 Introduction

Nowadays, periodic structures, such as electromagnetic bandgap (EBG) and frequency selective surface (FSS), have attracted much attention and have been applied to a variety of applications requiring very high performances. Indeed, they have been used in military domains, radar applications, wireless security, telecommunications and more particularly in antenna-based applications [1, 2]. Depending on their structures, their forms and dimensions, EBG and FSS exhibit wave propagation in special directions and for distinct frequencies. Therefore, they can be used as low-pass, high-pass, band-stop, or band-pass filters [2, 3]. For this reason, many researchers have interested in the use of multilayer as well as single-layer FSS structures for improving the performance of antennas in various narrowband and ultra-wideband (UWB) applications. In the scientific literature, it has been widely reported that the integrated FSS structures, with various antennas as a reflector or as a superstrate, increase significantly their gain, their directivity or impedance bandwidth and reduce their back-lobe radiation [4–12]. For example, in [4–6] the use of multilayer FSS, as baking reflector below UWB planar antenna has demonstrated $>3\,\text{dBi}$ gain enhancement. Also, in [7, 8], the authors have employed an FSS as a superstrate above a microstrip patch antenna to ameliorate its directivity (an improvement around $6\,\text{dBi}$ for [7] and $5\,\text{dBi}$ for [8]). In [9, 10], the reconfigurable antennas, based on a switchable active FSS for improving the impedance bandwidth and radiation pattern, have been proposed. A performance enhancement of these structures has been demonstrated with a maximum gain $>8\,\text{dBi}$ and a fractional bandwidth (FB) $\sim 8\%$. Likewise, the authors in [11] have proposed a dual-band FSS with double rectangular ring elements for improving impedance bandwidth of the microstrip slot antenna by around 2.37% at 2.45 GHz and only 2% at 5.8 GHz. At this time, a maximum gain around 5 dBi has been obtained.

Regarding the problem in how to redirect the back radiation and hence increasing the gain and directivity of microstrip antenna with wide impedance bandwidth, several techniques, based on the combination of FSS layer with other periodic structures such as metamaterial, FSS/EBG, FSS/AMC, or FSS/HIS, have been proposed in the literature. As examples, we can cite Jerusalem cross-shaped FSS (JC-FSS) used as an artificial magnetic conductor (AMC) ground plane [12], metamaterial reflective surface (MRS) used as a superstrate for a single-feed microstrip patch antenna [13], integrated metamaterial loading used in beam tilting antenna [14], high impedance surface (HIS) elements, with the modified FSS (MFSS), employed as superstrate of microstrip antenna [15] and FSS properties of a uni-planar EBG used as superstrate of microstrip antenna [16]. Several other complex structures, based on the use of only a simple FSS technique, have been also proposed in the literature to get a higher gain with a very wideband antenna. The latter ones, which consist of a multilayer FSS with various shapes and a large size unit cell, cause an increase in the cost and occupied space. For example, in [6, 17], the authors have proposed a wide impedance bandwidth antenna with reflector, having a maximum improvement gain $>3.5\,\text{dB}$. Nevertheless, the bulky space, caused by the use of multilayer FSS and a large dimension of the unit cell, lead to an increase in volume. Also, in [18], the design of slot antenna with multilayer FSS (as superstrate) has been presented. Indeed, despite that the latter structure offers a fractional bandwidth of 65% with the centre frequency of $6.5\,\text{GHz}$ and dimensions of $70\times 70\,\text{mm}^2$, it is limited by its high profile (29 mm). To remedy this problem, the design of a compact FSS layer, integrated with the rectangular slot antenna, offering a wideband (40% with the centre frequency of 10 GHz), and low profile, has been investigated in [19]. Yet, a gain enhancement of only 2.5 dBi in the direct line, compared to the measured gain of the antenna without FSS, is obtained.

Moreover, an interesting design of planer antenna with single-layer FSS proposed in [20] has provided a UWB spectrum and a high peak gain of 8.9 dBi with the unit cell dimensions of $16\times 16\,\text{mm}^2$. Despite this quality, this design is limited by its occupied total space that is $96\times 96\times 27\,\text{mm}^3$. It is therefore difficult to design a simple combined FSS-antenna structure using a compact single-layer FSS having best performances in terms of gain, impedance bandwidth, size and profile. To sum up, the given different structures have different major disadvantages.

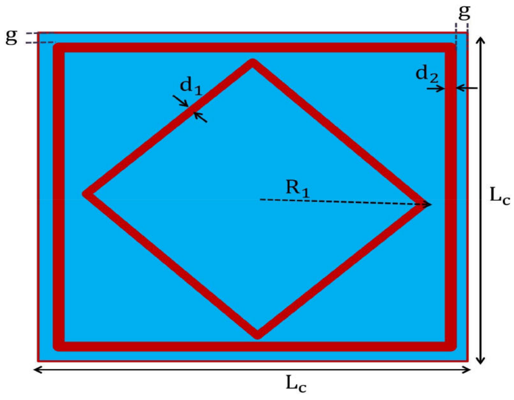

a

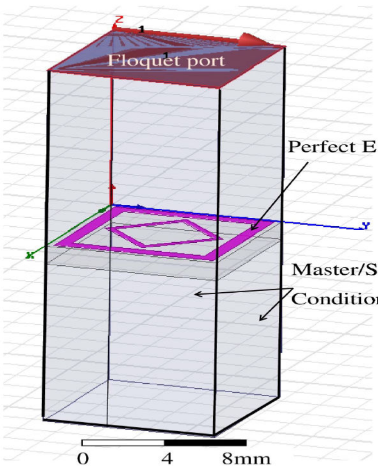

b

Fig. 1 *Geometry of the proposed FSS structure*
(a) One-unit cell, ***(b)*** Simulation setup of the unit cell in HFSS

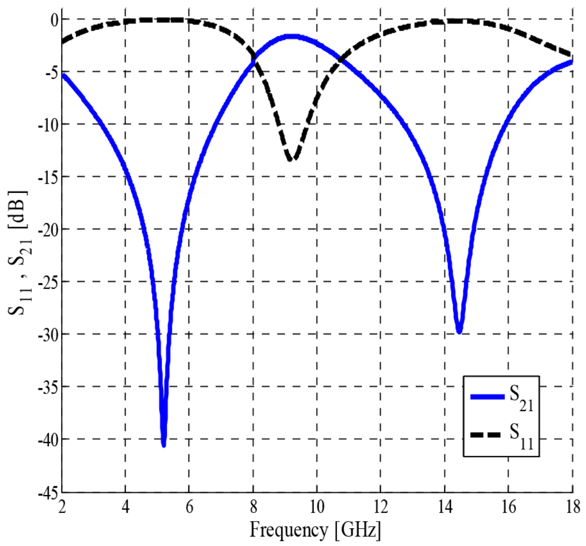

Fig. 2 *Transmission and reflection coefficients of the proposed FSS over UWB*

In this paper, a novel, simple design of wideband single-layer FSS, as a baking reflector of broadband planner slot antenna, is proposed. The latter structure, excited with a simple microstrip feed line, has a low profile, compact size, low cost and easy design. This proposed antenna with FSS reflector is designed and analysed by HFSS [21] and computer simulation technology (CST) Microwave Studio [22]. To validate the numerical results, the final combined design is fabricated and tested.

This paper is organised as follows: Section 2 presents the geometry and the analysis of FSS unit cells. In Section 3, the combination designs of the proposed antenna alone and its combinations with FSS and PEC (perfect electric conductor) reflectors together with the simulation results are reported. In Section 4, the experimental results of the fabricated structure are discussed. Finally, we end up with a conclusion.

2 FSS unit cell design

The proposed FSS structure is designed on a low-cost FR4 substrate with a thickness of 1.57 mm, a relative permittivity of 4.4 and a loss tangent equal to 0.02. This structure is similar to the unit cell of [11], but with modified dimensions and form of inner square loop. The unit cell is repeated periodically $n \times n$ times in each of the x and y directions with periodicity L_c to construct an FSS array that will be used as a reflector for the proposed wideband slot antenna. Both repetition and similarity make it possible to simplify the study of this complete $n \times n$ elements by analysing only a single unit cell. This is due to the fact that the calculated electromagnetic fields are similar in each unit cell. This last consists of two resonant metallic square-loop structures with different sizes and widths printed on the upper face of the dielectric substrate with no ground plane. The inner metallic square loop is oriented by 45° with respect to the outer square (see Fig. 1*a*). In this case, each metallic square resonates when its four sides measure about a quarter of the wavelength ($\lambda_0/4$) and one of them exhibits a stop-band response over the UWB. Accordingly, the combination of these two elements structures leads to the creation of a dual stop-band response.

In what follows, we will give the steps corresponding to the principle of the design of our proposed broadband planar slot antenna using a wide single-layer FSS stop-band reflector. In the first step, the unit cell is designed and simulated for dual wide stopbands using an analysis with Floquet port and periodic boundary conditions that are applied in CST Microwave Studio and HFSS simulators (see Fig. 1*b*). Fig. 2 shows the variation of the FSS's unit cell reflection and transmission coefficients versus frequency proving the dual stop-bands response. At this time, the inner square loop resonates at the higher frequency and exhibits an impedance bandwidth ranging from 3.2 to 6.8 GHz. The lower frequency is controlled by the outer square for the stopband from 12.8 to 15.9 GHz. The pass-band (corresponding to S_{11} less than -10 dB) between the two stopbands is controlled by the space separating the two structures (inner and outer squares) which depends on the diameter R_1, the thickness d_1 and d_2, and the gap between the cells.

In the second step, a study of a unit cell in the first stopband, which covers Wireless Local Area Network (WLAN), Worldwide interoperability for Microwave Access (WiMAX) and C bands, is presented. The latter bands correspond to the operating band of the proposed broadband antenna whose gain is to be enhanced. The performances, in terms of S-parameters magnitude and phase, of this unit cell in the normal incidence ($\theta = 0°$), are investigated as shown in Figs. 3 and 4. Fig. 3*a* displays the influence of the gap on the FSS cell unit transmission coefficient (S_{21}). Here, all parameters are kept constant and the parameter g is varied from 0.05 to 0.45 mm. From Fig. 3*a*, it can be seen that the resonance frequency band extends to the higher frequency region. In the other hand, as shown in Fig. 3*b*, the reflection phase of the FSS, for different values of g, decreases with the increase of the frequency. Nevertheless, the zero reflection phase changes to the higher frequency region. In addition, the resonance frequency of the stop-band unit cell is affected by the periodicity L_c, leading to the variation of electric length of the unit cell, as mentioned in the first paragraph of this section. As illustrated in Fig. 4, it can be observed that, when the periodicity varies from 8 to 11 mm, the resonance frequency is shifted to the lower frequency region and the stopband is narrowed. As reported previously, the realised intensive parametric study proves that the frequency response of the unit cell stopband is affected by several parameters such as the periodicity L_c and the gap g. Moreover, other parameters such as the widths d_1 and d_2 of the two metallic square rings and R_1 have an influence on the FSS stop-band response. Therefore, simultaneous optimisation

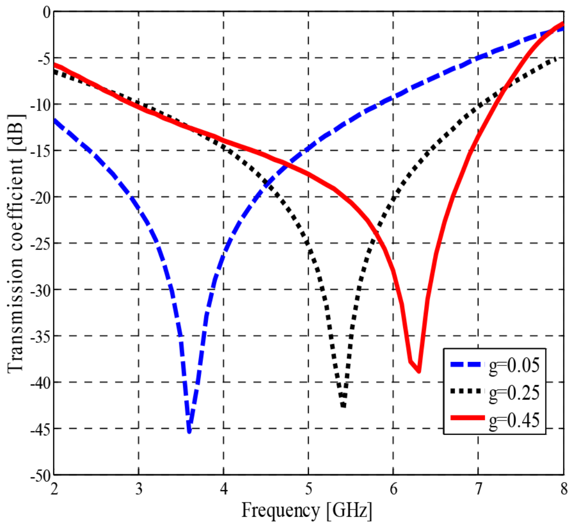

a

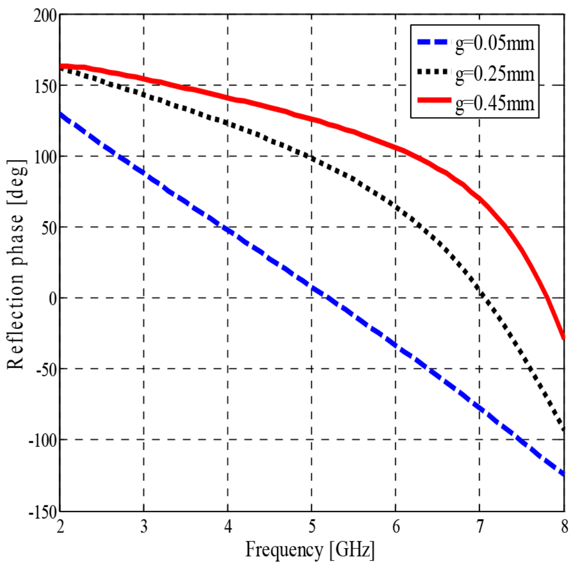

b

Fig. 3 *Variation of S-parameters of the unit cell for different gap values*
(a) Transmission coefficient; ***(b)*** Reflection phase

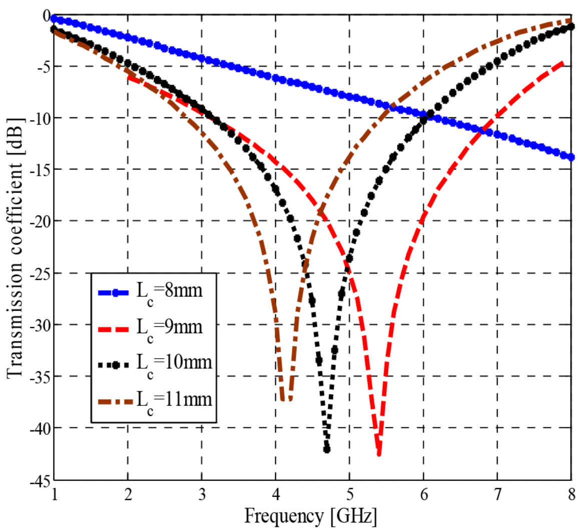

Fig. 4 *Variation of the transmission coefficient of the proposed FSS for different values of periodicity*

of all dimension parameters is required and carried out using Optimetrics Toolbox of HFSS for wide stopband (transmission coefficient ≤ −10 dB). The optimised parameters of the one-unit

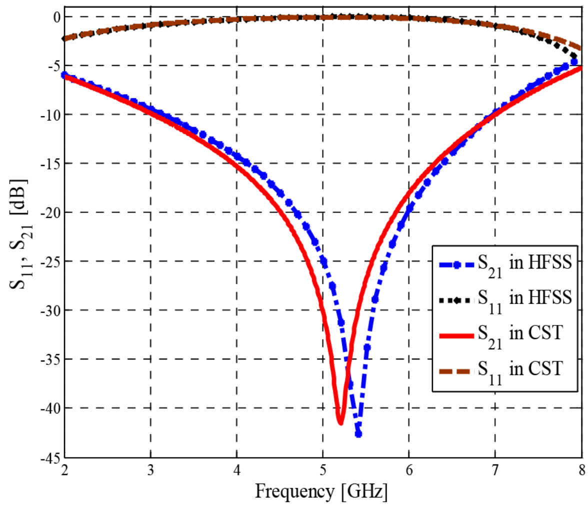

Fig. 5 *Reflection and transmission coefficients of the optimised FSS unit cell*

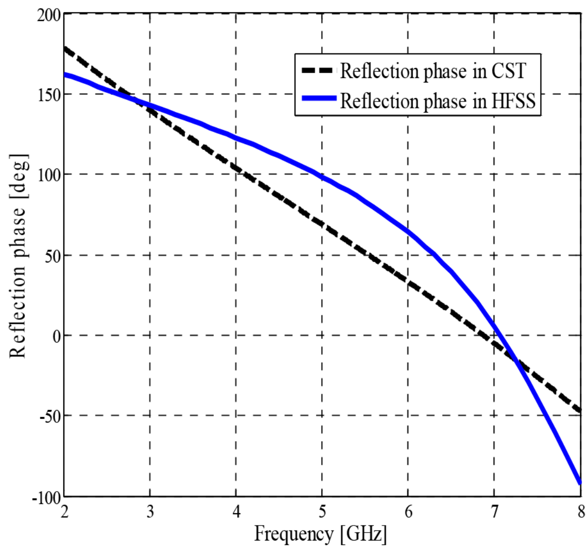

Fig. 6 *Variation of the reflection phase of the optimised FSS unit cell versus frequency*

cell are given as follows: $R_1 = 2.6$ mm, $d_1 = 0.5$ mm, $L_c = 9$ mm, $g = 0.25$ mm, $d_2 = 0.8$ mm.

As shown in Fig. 5, the optimised design of the unit cell resonates around 5.4 GHz, giving a transmission coefficient (S_{21}) of −43.5 dB. The stop-band bandwidth (for S_{21} less than −10 dB) is ∼ 4 GHz, which represents 80% with respect to the 5 GHz centre frequency.

Fig. 6 indicates that the optimised unit cell offers a phase that decrements with the augmentation of the frequency in the whole operating bandwidth (from 3 to 7 GHz). This result represents the ideal case that can be used in the antenna-gain enhancement. In fact, it can exhibit constructive interference with the antenna back radiated waves. It can be clearly seen, from Figs. 6 and 7, that the HFSS simulated results are in good agreement with those of CST. The slight difference between them is probably due to using of different computational techniques in these two simulators (finite integration technique (FIT) in CST and FEM in HFSS).

3 Antenna integration with FSS

For the purpose of studying the gain enhancement of the wideband slot antenna, FSS structure is integrated within this latter to get a combined structure. The resultant structure is then compared with an antenna incorporating a PEC reflector. Before proceeding to this step, a simple aperture planner antenna is designed and optimised, for miniaturised size and wide bandwidth, using the FR4 epoxy substrate with a thickness of 1.57 mm, a relative permittivity of 4.4

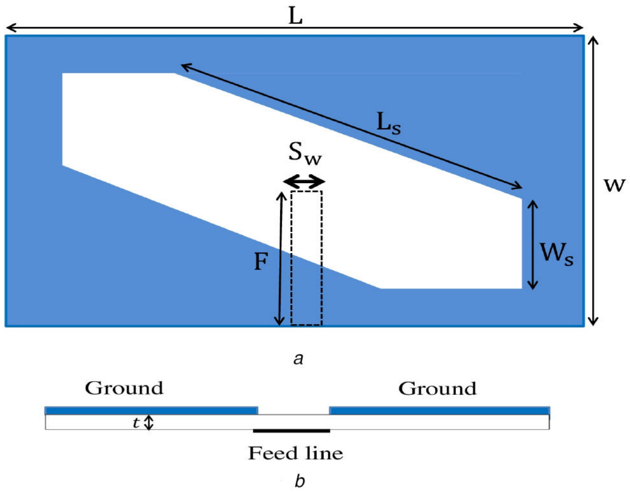

Fig. 7 *Geometry of the proposed slot antenna*
(a) Top view, ***(b)*** Side view

and a loss tangent of 0.02. The slot is etched on the ground plane that has the dimension of $L \times w$, printed on the top side of the substrate. The structure excitation is ensured by a rectangular microstrip feed line, of width S_w and length F, that is printed on the other side (bottom) of the substrate. As depicted in Fig. 7, the slot has four sides each having a length equal to W_s and two equal sides with L_s length each. The FSS structure is placed under the slot antenna with optimal distance H as shown in Fig. 8*b*.

It has been found that the antenna gain in the presence of FSS reflector will be optimal whenever the reflected back radiated waves, from the antenna towards FSS ($\varnothing_b$), and the reflected waves, from the FSS reflector ($\varnothing_r$) in the R-plane, are added in phase, which provokes a rising of constructive interference [6]. The total phase at reference T-plane can be obtained by the following equation:

$$\varnothing_T = \varnothing_r + \varnothing_b \tag{1}$$

with

$$\varnothing_b = 2\frac{2\pi f}{C}H \tag{2}$$

where C is the celerity of light.

As shown in Fig. 8*b*, the antenna back radiated waves $\varnothing_b$ are reflected. These reflexions increase with the augmentation of the frequency and are controlled by the height H, as illustrated in (2). Note that the coherence phase is obtained when $\varnothing_T$ becomes a multiple of 2π. This can be given as follows:

$$\varnothing_T = 2\pi n \tag{3}$$

with $n = 0, 1, 2, \ldots$

In this case, the ideal FSS phase reflection $\varnothing_r$ must diminish with the increase of frequency. As an effect, it compensates the rise of $\varnothing_b$ and provokes the increase of directivity and gain of slot antenna.

In order to achieve high performances, in terms of impedance bandwidth and gain with the miniaturised size of the antenna with reflector (number of unit cells n), all parameters of the antenna with FSS need to be optimised. The optimal parameters dimensions, in mm, are given as follows: $w = 24$, $L = 29$, $W_s = 7.32$, $L_s = 16.8$, $F = 16$, $S_w = 2$, $H = 12$, $g = 0.3$, $d_2 = 1$, $d_1 = 0.5$, $L_c = 9$, $R_1 = 2.6$, with $n \times n = 49$ cells $= 63 \times 63\,\text{mm}^2$.

The performances of the optimised slot antenna alone are compared with those of its combination with FSS and its combination with PEC. Fig. 9 shows the variation of the reflection coefficient of slot antenna alone, the slot antenna with FSS and the slot antenna with PEC. From this figure, it can be noted that the

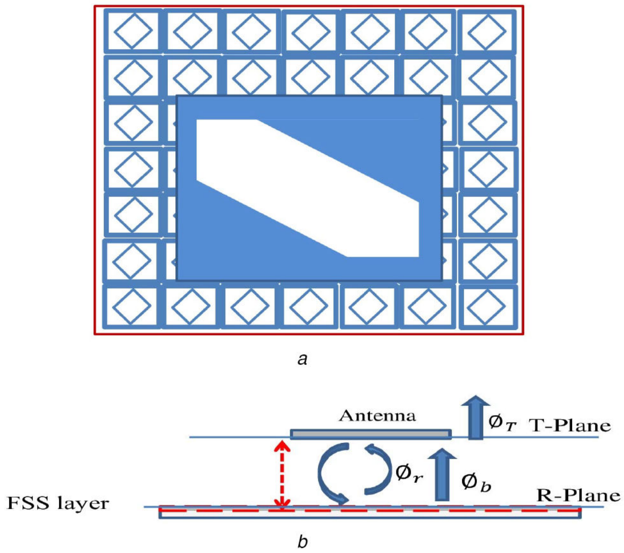

Fig. 8 *Geometry of the optimised slot antenna with FSS (49 cells)*
(a) Top view, ***(b)*** Side view with operation mechanism of reflected and transmitted waves

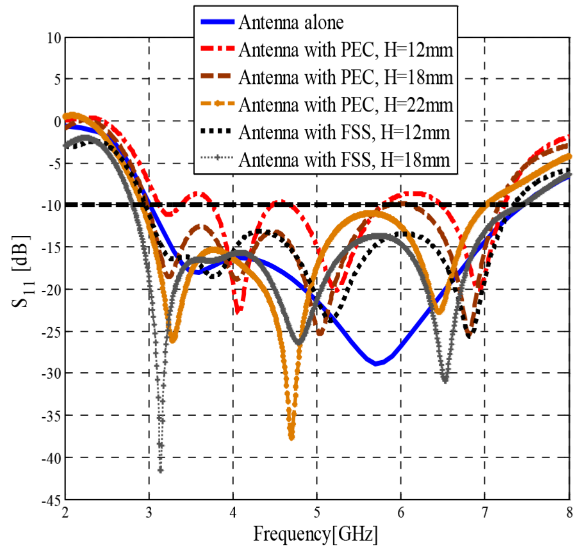

Fig. 9 *Reflection coefficients of different combinations of antenna for different values of height H*

FSS and PEC reflectors have an influence on the level and the form of the reflection coefficient. However, a very slight influence is observed over the total impedance bandwidth, which is 4.3 GHz (83.49%) for an antenna with FSS reflector ($H = 0.12\lambda_0$) and 4.4 GHz (84.61%) for antenna alone. On the other hand, the fractional bandwidth of 80% (4 GHz from 3 to 7 GHz), for PEC reflector placed at a height $H = 22\,\text{mm} \simeq \lambda_0/4$, is obtained. Note here that the impedance bandwidth is reduced and deteriorated by using an H value that is less than $\lambda_0/4$. As a consequence, increasing the height of the antenna above the PEC or FSS improves the impedance bandwidth, but a compromise should be made between the antenna compactness and the volume.

The so obtained realised gain versus frequency (at broadside direction $\varphi = 0°$, $\theta = 0°$), for an antenna with PEC, an antenna with FSS and antenna alone, is plotted in Fig. 10. From these curves, it can be seen that the FSS and PEC reflectors improve the average antenna gain in all frequency ranges. However, referring to Fig. 10 and Table 1, the comparison between the three cases indicates clearly that the FSS layer integrated with a slot antenna with a narrower height ($H = 0.12\lambda_0$) achieves a higher gain exceeding 9 dBi for the WLAN frequency band between 5.2 and 5.8 GHz. The same antenna over PEC reflector, with $H = \lambda_0/4$, achieves a maximum gain of 6.81 dBi at 4.8 GHz.

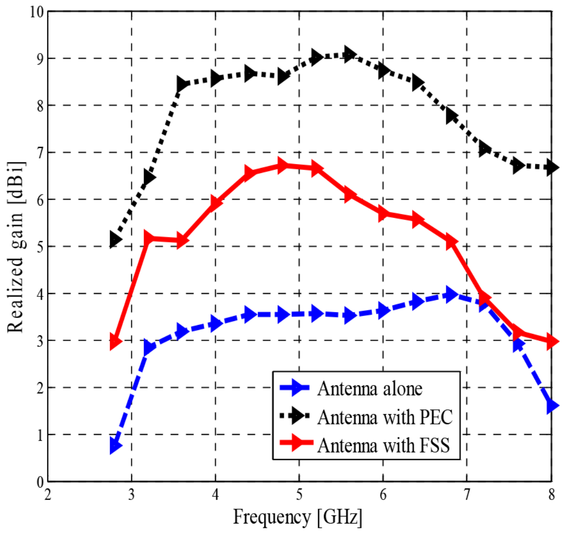

Fig. 10 *Variation of the realised gain for different combinations of antenna*

Table 1 Gain improvement of different combinations of antenna

Freq., GHz	Antenna with PEC, $H =$ 22 mm	Antenna with FSS, $H =$ 12 mm
	Gain improvement, dBi	
3.2	2.16	3.60
3.6	1.94	5.26
4.8	3.27	5.06
5.2	3.09	5.51
6.0	2.07	5.18
6.8	1.12	3.81

However, the antenna without reflector achieves a maximum gain of 3.97 dBi at 6.8 GHz. Yet, maximum gain improvement around 5.51 dBi at 5.8 GHz and 3.27 dBi at 4.8 GHz is achieved by using FSS and PEC reflectors, respectively.

4 Measurement results and discussion

The proposed structure was fabricated using PCB (printed circuit board) technology, where the slot antenna and the FSS reflector were fabricated separately and then combined by foam spacers. Fig. 11 depicts a photograph of the fabricated prototype antenna. The performances of the antenna alone and the antenna with FSS were simulated and measured. The measured *S*-parameters of the prototype antenna were carried out by Agilent Vector Network Analyser N5224A and the radiation patterns and gain were measured in an anechoic chamber. From Fig. 12, it can be noted that the measured −10 dB impedance bandwidth is 86.38% (from 2.92 to 7.36 GHz) for the structure with FSS and 85.71% (from 2.96 to 7.4 GHz) for that without FSS. It can be concluded that the simulated results are in good conformity with the measured ones. In addition, the measured gains of both structures, at different frequencies in the broadside direction ($\varphi = 0°$, $\theta = 0°$), were calculated as follows [14]:

$$G_x = G_{\text{ref}} + 10\log\left(\frac{P_x}{P_{\text{ref}}}\right) \quad (4)$$

Here G_x is the gain of the antenna under test (proposed slot antenna with and without reflector), and G_{ref} is the gain of the reference antenna.

The measured gain can be obtained by comparing the radiated power of the antenna under test and the reference antenna's power in the receiving mode, which are represented by P_x and P_{ref}, respectively. Furthermore, the obtained measured peak gain of the proposed antenna with and without FSS reflector is depicted in

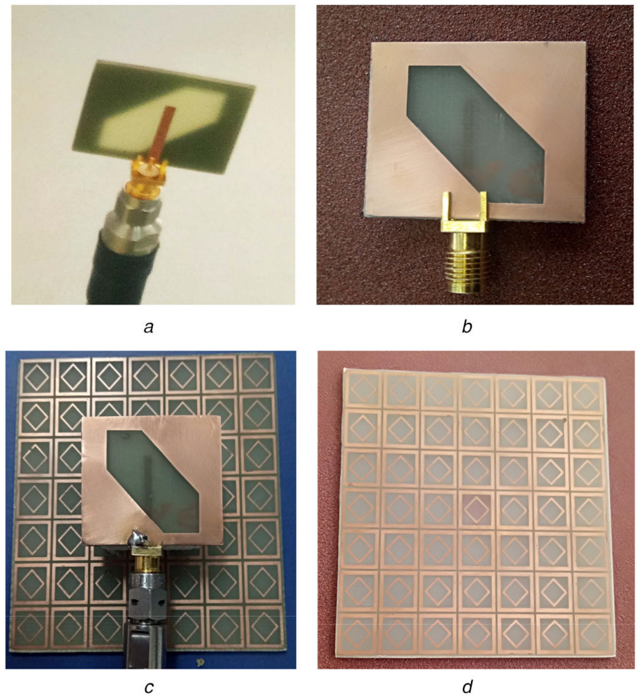

Fig. 11 *Fabricated prototypes*
(a), ***(b)*** Slot antenna bottom and top view, ***(c)*** Slot antenna with proposed FSS reflector excited by SMA connector, ***(d)*** FSS reflector

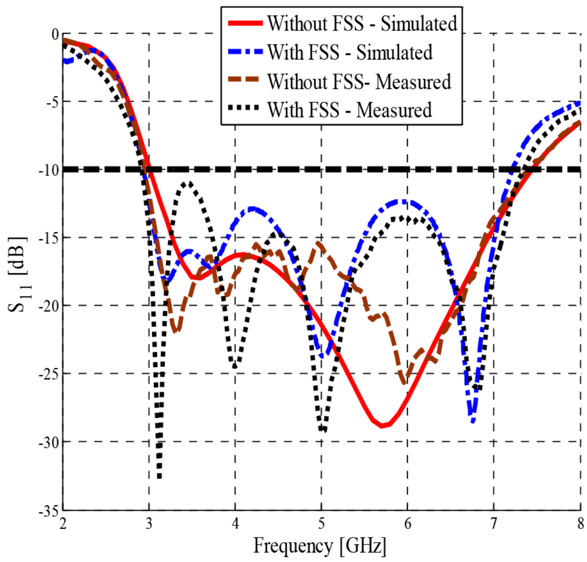

Fig. 12 *Measured and simulated reflection coefficients of the antenna with and without FSS*

Fig. 13. The comparison between simulated and measured results is summarised in Table 2. As indicated in this table, the measured maximum gain of both antennas with FSS and without FSS is 8.87 dBi at 5.2 GHz and 3.55 dBi at 6 GHz, respectively. Hence, the maximum gain enhancement of 5.53 dBi at 5.8 GHz is achieved using the FSS reflector. The simulated results indicate that the proposed antenna provides a maximum gain of 9.06 dBi in the band between 5.2 and 5.8 GHz, which leads to a maximum gain improvement of 5.51 dBi compared to the antenna without FSS. The comparison between the simulated and measured results shows a good agreement.

Moreover, the radiation patterns for both structures are simulated and validated by measurements in an anechoic chamber for the *E*-plane (*YZ*) and *H*-plane (*XZ*) at several frequencies, including 4, 5.2 and 5.8 GHz, as plotted, respectively, in Figs. 14–16. The obtained results indicate that the normalised radiation patterns, without FSS, are bidirectional in the *E*-plane and quasi-omnidirectional in the *H*-plane. After the application of FSS

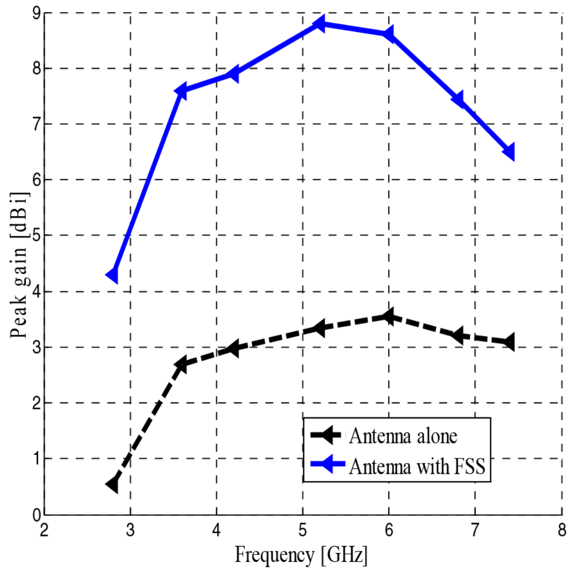

Fig. 13 *Measured peak gain of the antenna with and without FSS*

Table 2 Simulated and measured antenna gains at different frequencies

Freq.,GHz	Simulated antenna	Measured antenna	Simulated antenna with FSS	Measured antenna with FSS
	Gain, dBi			
2.8	0.74	0.55	5.13	4.30
3.6	3.17	2.70	8.43	7.60
4.2	3.5	2.98	8.86	7.90
5.2	3.54	3.34	**9.06**	**8.87**
6	3.62	**3.55**	8.8	8.60
6.8	**3.97**	3.2	7.78	7.43
7.4	3.7	3.1	7.00	6.50

structure, more particularly at band between 5.2 and 5.8 GHz, the radiation patterns became more directional and the back lobes are minimised by > 15 dBi. Also, it can be seen that the pattern of the antenna with FSS, at 4 GHz (lower frequency) in *H*-plane, keeps nearly the same curve compared to that without FSS. This is due to the fact that the antenna radiation is affected by different parameters such as linearly decreasing phase as well as the size of the FSS reflector. As a consequence, the radiation can be further improved, especially at a lower frequency, by increasing the size of the FSS reflector (cells number) which is undesirable because it increases the size of the antenna. Furthermore, the comparison between the simulated and measured results regarding the gain and radiation patterns of both structures reveals a good agreement. The slight difference between the measured and simulated results is probably due to fabrication constraints, such as the quality of the SMA connector, uncertainties in the dielectric permittivity, the thickness of FR4 substrate, foam spacer and the mismatch between the slot antenna and the FSS layer.

The proposed antenna is compared with the most relevant of those reported in the literature, and the results are summarised in Table 3. As exposed in this table, the proposed structure exhibits a better characteristic in terms of size, profile, gain enhancement and bandwidth rather than those presented in [18, 19, 15]. However, in [16] the directivity improvement of 6.9 dBi is achieved at 10.8 GHz, but with a high profile and an insignificant bandwidth (5.5%). Furthermore, in [7] the aperture-coupled microstrip antenna (ACMA) with FSS superstrate provides a directivity enhancement of 6 dBi at 9.5 GHz, but it has a high back lobe and a high profile with 34.6% of impedance bandwidth. In addition, four vertical layers metamaterial slabs and curved reflector are used in [14, 23], respectively. The antennas resulting from the latter structures are more complex with 3D design, while the proposed structure shows a better gain, larger bandwidth and less complexity in terms of fabrication.

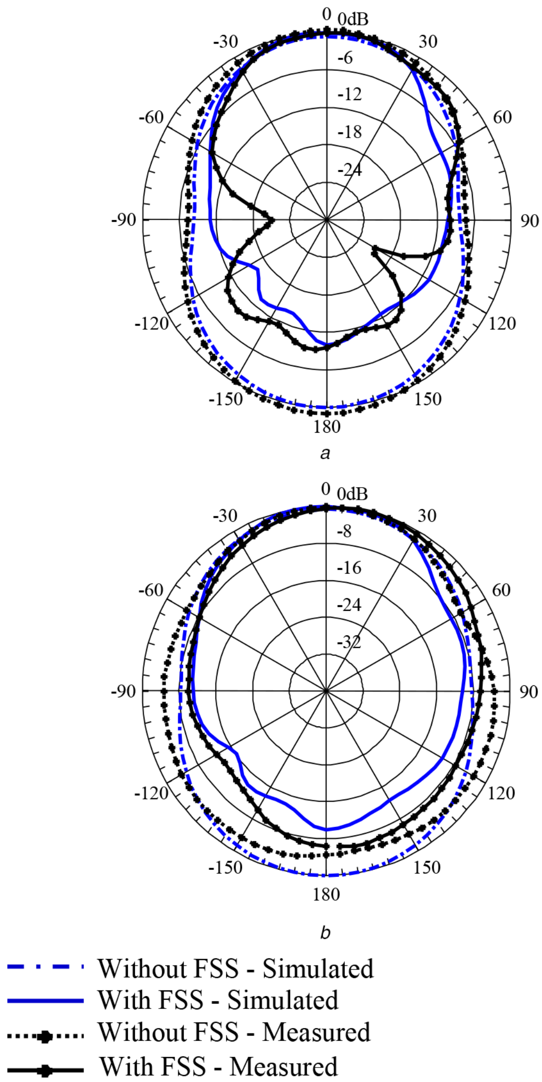

Fig. 14 *Measured and simulated Radiation patterns of the antenna with and without FSS for* $f = 4$ GHz
(a) *E*-plane, ***(b)*** *H*-plane

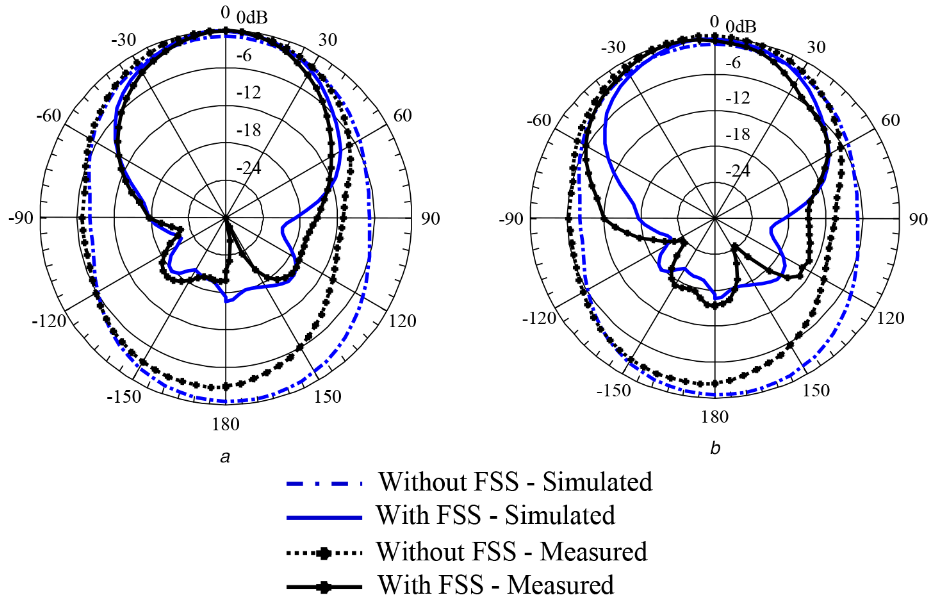

Fig. 15 *Measured and simulated radiation patterns of the antenna with and without FSS for* $f = 5.2\,\text{GHz}$
(a) *E*-plane, ***(b)*** *H*-plane

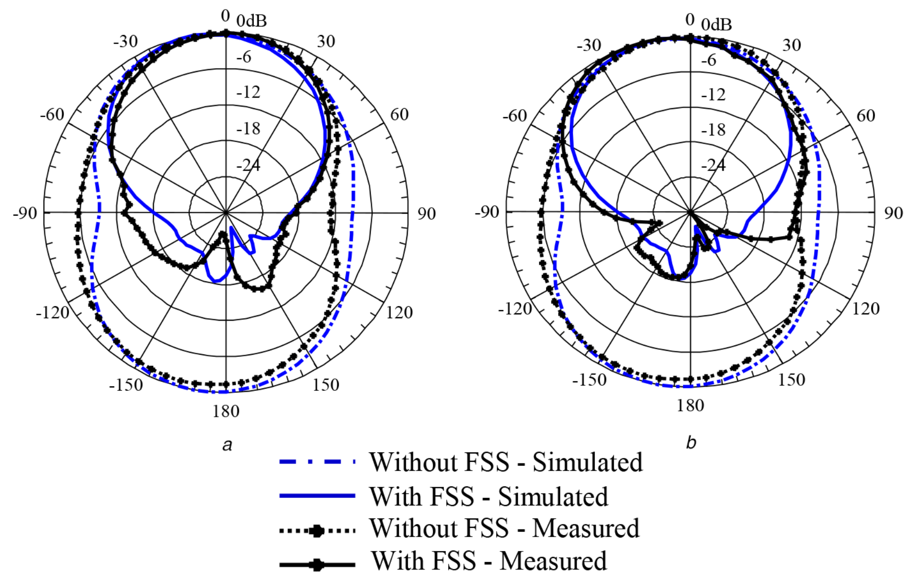

Fig. 16 *Measured and simulated radiation patterns of the antenna with and without FSS for* $f = 5.8\,\text{GHz}$
(a) *E*-plane, ***(b)*** *H*-plane

Table 3 Comparison between the proposed antenna and the most relevant of those reported in the literature

Ref.	C. Freq.,GHz	Profile, λ_0	FB, %	Gain improvement, dBi
[19]	8	0.47	40	2.5
[18]	6.5	0.63	65	4.0
[14]	7.5	/	13.33	2.73
[15]	2.45	0.22	4.89	5 in directivity
[16]	10.8	0.52	5.5	6.9 in directivity
[7]	8.6	0.52	34.6	6 in directivity
[23]	5.5	0.18	18	5.5
this work	5.14	0.12	86.38	5.53

5 Conclusion

In this paper, a simple wideband antenna with compact FSS reflector has been designed, simulated, and validated by measurements. The obtained results have shown a great concordance between the simulations and measurements and proved that the proposed antenna is able to offer good performances for wideband applications ranging from 2.92 to 7.36 GHz (86.38% referenced to the 5.14 GHz centre frequency). Besides, the average gain has been enhanced by using the proposed FSS reflector. In fact, a gain improvement of 5.5 dBi and a maximum measured gain of 8.87 dBi is provided for the proposed structure. In addition, the latter one has achieved directional radiation with reduced back lobes levels by > 15 dBi in the WLAN band. As a consequence, the proposed combination can be a good candidate for several services of wireless communication systems, including WiMAX ((3.2 – 3.8 GHz)), C band for satellite applications (3.7 – 4.2 GHz), and WLAN band (5.15 – 5.85 GHz).

In general, this antenna can be useful in applications requiring broadband antennas with high gain, miniaturised size, and low profile.

6 References

[1] Mias, C., Tsokonas, C., Oswald, C.: '*An investigation into the feasibility of designing frequency selective windows employing periodic structures*' (The Nottingham Trent University, Burton Street, Nottingham, NG1 4BU, UK, 2002)

[2] Munk, B.A.: '*Frequency selective surfaces: theory and design*' (Wiley, New York, 2000)

[3] Wu, T.K.: '*Frequency selective surface and grid array*' (Wiley, New York, 1995)

[4] Ranga, Y., Esselle, K. P., Matekovits, L., *et al.*: 'Increasing the gain of a semi-circular slot UWB antenna using an FSS reflector'. Proc. Int. Conf. IEEE APS Topical Conf. on Antenna and Propagation in Wireless Communication (APWC), Cape Town, September 2012, pp. 478–481

[5] Ram Krishna, R.V.S., Kumar, R.: 'Slotted ground microstrip antenna with FSS reflector for high-gain horizontal polarization', *IET Electron. Lett.*, 2015, **51**, (8), pp. 599–600

[6] Ranga, Y., Matekovits, L., Esselle, K.P., *et al.*: 'Multioctave frequency selective surface reflector for ultra-wide band antennas', *IEEE Antenna Wirel. Propag. Lett.*, 2011, **10**, pp. 219–222

[7] Pirhadi, A., Bahrami, H., Nasri, J.: 'Wideband high directive aperture coupled microstrip antenna design by using a FSS superstrate layer', *IEEE Trans. Antennas Propag.*, 2012, **60**, (4), pp. 2101–2106

[8] Pirhadi, A., Keshmiri, F., Hakkak, M., *et al.*: 'Analysis and design of dual band high directive EBG resonator antenna using square loop FSS as superstrate layer', *Prog. Electromagn. Res.*, 2007, **70**, pp. 1–20

[9] Mahmood, S.M., Denidni, T.A.: 'Pattern reconfigurable antenna using a switchable frequency selective surface with improved bandwidth', *IEEE Antenna Wirel. Propag. Lett.*, 2015, **99**, pp. 1148–1151

[10] Tsai, Y.L., Hwang, R.B., Lin, Y.D.: 'A reconfigurable beam-switching antenna base on active FSS'. Proc. 15th Int. Symp. Antenna Technology and Applied Electromagnetic (ANTEM), Toulouse, France, August 2012, pp. 1–4

[11] Chen, H.Y., Tao, Y.: 'Bandwidth enhancement of a U-slot patch antenna using dual-band frequency-selective surface with double rectangular ring elements', *Microw. Opt. Technol. Lett.*, 2011, **53**, (7), pp. 1547–1553

[12] Monavar, F.M., Komjani, N.: 'Bandwidth enhancement of microstrip patch antenna using Jerusalem cross-shaped frequency selective surfaces by invasive weed optimization approach', *Prog. Electromagn. Res.*, 2011, **121**, pp. 103–120

[13] Chaimool, S., Chung, K.L., Akkaraekthalin, P.: 'Simultaneous gain and bandwidths enhancement of a single-feed circularly polarized microstrip patch antenna using a metamaterial reflective surface', *Prog. Electromagn. Res. B*, 2010, **22**, pp. 23–37

[14] Dadgarpour, A., Zarghooni, B., Virdee, B.S., *et al.*: 'Beam tilting antenna using integrated metamaterial loading', *IEEE Trans. Antennas Propag.*, 2014, **62**, (5), pp. 2874–2879

[15] Arnmanee, P., Phongcharoenpanich, C.: 'Improved microstrip antenna with HIS elements and FSS superstrate for 2.4 GHz band applications', *Int. J. Antennas. Propag.*, 2018, **2018**, pp. 1–11

[16] Kurra, L., Abegaonkar, M.P., Basu, A., *et al.*: 'FSS properties of a uniplanar EBG and its application in directivity enhancement of a microstrip antenna', *IEEE Antennas Wirel. Propag. Lett.*, 2016, **15**, pp. 1606–1609

[17] Ranga, Y., Matekovits, L., Weily, A.R., *et al.*: 'A constant gain ultra-wideband antenna with multi-layer frequency selective surface', *Prog. Electromagn. Res. Lett.*, 2013, **38**, pp. 119–125

[18] Chatterjee, A., Parui, S. K.: 'Gain enhancement of a wide slot antenna using a second-order band pass frequency selective surface', *Radioengineering*, 2015, **24**, (2), pp. 455–461

[19] Moharamzadeh, E., Javan, A.M.: 'Triple-band frequency selective surfaces to enhance gain of x-band triangle slot antenna', *IEEE Antennas Wirel. Propag. Lett.*, 2013, **12**, pp. 1145–1148

[20] Tahir, F.A., Arshad, T., Ullah, S., *et al.*: 'A novel FSS for gain enhancement of printed antennas in UWB frequency spectrum', *Microw. Opt. Technol. Lett.*, 2017, **59**, (10), pp. 2698–2704

[21] Ansys, High Frequency Structure Simulation (HFSSTM), Ver. 15. Available at: http://www.ansys.com

[22] CST Microwave Studio Computer Simulation Technology. Available at: http://www.cst.com.2015

[23] Park, J.S., Choi, H.K.: 'The design of the dual band folded dipole antenna with a parabolic curved reflector', *Microw. Opt. Technol. Lett.*, 2019, **61**, (5), pp. 1419–1424